International Conference on Space Optics—ICSO 2014

La Caleta, Tenerife, Canary Islands

7–10 October 2014

Portable traceability solution for ground-based calibration of optical instruments

Omar El Gawhary

Marijn van Veghel

Pepijn Kenter

Natasja van der Leden

et al.

PORTABLE TRACEABILITY SOLUTION FOR GROUND-BASED CALIBRATION OF OPTICAL INSTRUMENTS

Omar el Gawhary[1], Marijn van Veghel[1*], Pepijn Kenter[2], Natasja van der Leden[1], Paul Dekker[1], Elena Revtova[1], Maurice Heemskerk[1], André Trarbach[1], Ramon Vink[3], Dominic Doyle[3]

[1] VSL, Delft, The Netherlands; [2] Science and Technology B.V., Delft, The Netherlands; [3] ESA ESTEC, Noordwijk, The Netherlands

*Corresponding author: VSL, P.O. Box 654, 2600 AR Delft, The Netherlands; mvveghel@vsl.nl

Abstract – **We present a portable traceability solution for the ground-based optical calibration of earth observation (EO) instruments. Currently, traceability for this type of calibration is typically based on spectral irradiance sources (e.g. FEL lamps) calibrated at a national metrology institute (NMI). Disadvantages of this source-based traceability are the inflexibility in operating conditions of the source, which are limited to the settings used during calibration at the NMI, and the susceptibility to aging, which requires frequent recalibrations, and which cannot be easily checked on-site. The detector-based traceability solution presented in this work uses a portable filter radiometer to calibrate light sources on-site, immediately before and after, or even during instrument calibration. The filter radiometer itself is traceable to the primary standard of radiometry in the Netherlands. We will discuss the design and realization, calibration and performance verification.**

I.   INTRODUCTION

The accuracy of optical instruments that are used on board of earth observation (EO) satellites has direct impact on the quality of the data obtained with them, and on the validity of the conclusions drawn from that data [1]. For this reason, considerable effort is spent on the radiometric calibration of these instruments before flight. The goal of these calibrations is to establish a link between the instrument readings and the relevant units within the International System of Units (SI) [2]. The term which expresses the existence of such a link is traceability. In order to achieve traceability, reference standards have to be used which are themselves traceable to the SI. This means that these reference standards are – directly or indirectly – calibrated against the primary realization of the SI units at a national metrology institute (NMI).

For optical calibrations, the reference standards frequently take the form of calibrated lamps. FEL lamps with an NMI calibrated spectral irradiance can be used as spectral irradiance standards, to calibrate the spectral irradiance response of an EO instrument. They are however not very flexible: the distance and current setting have to be identical to the distance and current setting during calibration at the NMI, leaving no room for adapting the irradiance level. Moreover, the calibration is only valid for a limited number of burning hours. Recalibration, or even an intermediate check, can only be performed by sending the lamp back to the NMI. This results in loss of time, with the consequence that recalibration will not be performed as frequently as is perhaps desired. In between recalibrations, only assumptions can be made regarding the drift behaviour of the lab, with no way of directly checking these assumptions.

No reference standard used for transferring traceability is completely immune to drift, but there are important variations in the level of long-term stability that can be achieved. With a detector-based traceability solution, a much greater stability is possible. Also, detectors with good linearity over a large range can be realized, providing a higher degree of flexibility. In this scheme, a source will still be necessary for calibration of EO instruments, but instead of making the source the carrier of the traceable scale, this scale is incorporated into a portable detector. The detector allows for the on-site calibration of the source, immediately before and after the source is used for the calibration of the EO instrument. The source calibration can be done with exactly the settings needed for the instrument calibration and where necessary, intermediate checks are possible.

The most accurate radiometric detectors are electrical cryogenic substitution radiometers (ESCRs) [3-5], used in combination with a tuneable light source to realize a spectral irradiance scale. These types of detectors are indeed used at NMIs as primary standards. They are however inherently slow, bulky and require cryogenic cooling, making them unsuited as a portable standard. Solid-state detectors made of e.g. Si, Ge or InGaAs (depending on the desired wavelength range) are more compact and are successfully being used as transfer detectors, in particular in a so-called trap configuration [6]. In a trap detector, several detectors are

arranged in series, so that light reflected from the first detector hits the second detector and so on. The total reflection from such a trap detector is well below 1%. For a given wavelength, a trap detector shows excellent linearity over a large spectral irradiance range, as well as a high degree of polarization insensitivity.

To measure spectral irradiance, a wavelength selection mechanism has to be provided. A scanning monochromator, as typically used with an ESCR, is to slow and bulky for a portable system. An alternative is to use a series of narrow band-pass filters to build a filter radiometer [7-11]. A filter radiometer measures the integrated spectral irradiance in a series of narrow bands. If the general shape of the spectrum is known, the spectral irradiance at other wavelengths can be obtained by model-based interpolation. Obviously, this procedure works best for relatively smooth spectra, which have no sharp features in between filter bands. Planckian, or quasi-Planckian spectra, such as those of a FEL lamp, are ideal in this regard.

A filter radiometer using solid state (trap) detectors is thus a good choice for a portable spectral irradiance scale to be used in combination with a FEL lamp as a calibration stimulus. In section II below, we will present our design for such a portable filter radiometer. In section III we will describe how the realized filter radiometer has been calibrated using our scanning spot method. The interpolation method used for constructing a continuous spectrum from the detector response for each of the individual filters will be discussed in section IV. Section V will show the results of a performance verification based on measurements of actual FEL lamps. We end with a conclusion and outlook in section VI.

II.   HARDWARE DESIGN AND REALIZATION

The filter radiometer contains three essential elements that together incorporate the portable spectral irradiance scale: (1) a series of filters to select different wavelengths; (2) a detector to measure the optical power transmitted by the filters; and (3) a precision aperture to define the effective area. An important design choice is the wavelength range over which the filter radiometer will operate. The wavelength range targeted in future EO missions (Tropomi, Sentinel 4 and 5) is 270—2400 nm. It is not possible to cover this entire wavelength range with a single solid-state detector. For this reason, the entire wavelength range is split up into three subranges, that will each be covered by a separate detector. An overview of this division is given in table 1. Per detector there is a dedicated set of filters spanning the specific wavelength range. These filters are placed in a filterwheel so that they can be rotated in front of the detector one-by-one. Each detector has its own precision aperture. The combination of precision aperture, detector, filterwheel and housing forms a modular unit, which we will call a detector-filter unit (DFU). A schematic drawing of such a DFU is shown in Fig. 1.

The filter wheel houses up to sixteen ½ inch filters. One filter position however has to be reserved for an internal shutter to measure the dark current. The diameter of the precision aperture is 3.5 mm. The current from the detector is converted by a trans-impedance amplifier on the DFU itself to a voltage in the range of 0 to 10 V. The DFU housing is made of black anodized aluminium. The temperature inside the housing is controlled by a combination of resistive heating elements and PT100 temperature sensors to ± 0.1 °C.

The entire filter radiometer features a carousel where three DFUs can be mounted, as shown in Fig. 2. In the current situation, only the UV-VIS DFU has been implemented. The NIR and SWIR DFUs can be easily added once they are realized. The carousel rotates the selected DFU in front of the opening in the filter radiometer housing. Note that the opening aperture in the filter radiometer housing is not the defining aperture for the spectral irradiance response; that is the aperture on the DFU. In fact, all elements that determine the spectral responsivity of the filter radiometer in a specific subrange are located within the respective DFU, making it sufficient to calibrate just the DFUs as independent elements.

Subrange	Wavelength interval	Detector type
UV-VIS	270—900 nm	Si trap detector
NIR	900—1600 nm	Ge trap detector
SWIR	1600—2400 nm	InGaAs photodiode

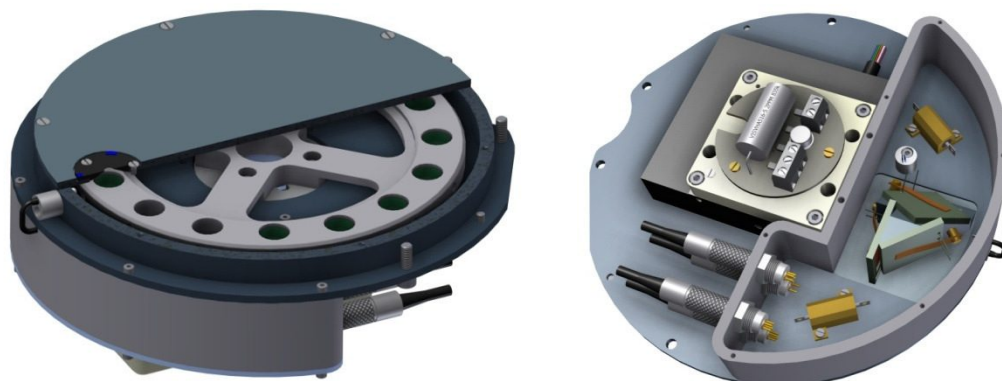**Table 1.** Wavelength subranges and detector types

Fig. 1. DFU design, seen from the front side where the light is incident (left) and from the back side (right). Depicted is the DFU for the UV-VIS subrange, which features a Si trap detector.

The filter radiometer housing fully covers the DFU carousel. It provides mechanical stability and thermal isolation. At the front of the housing there is a kinematic mount to place an alignment target over the entrance aperture. The filter radiometer itself rests on a tripod via another kinematic mount. Adjustment screws allow for precise alignment of the filter radiometer optical axis with respect to the source and the EO instrument under test. Because of the kinematic mount, the filter radiometer can be moved in and out of the optical path in a reproducible manner, allowing frequent monitoring of the source used as a stimulus. The distance to the source can be determined via a precision reference plane just below the entrance aperture, which has a calibrated offset with respect to the plane of the precision aperture of the DFU. The electronics are fitted together into one separate box, so that the whole setup can be transported and installed with ease. The whole system can be controlled remotely from a laptop connected through an Ethernet cable. Fig. 3 shows a photograph of the complete realized system.

Fig. 2. The DFU carousel inside the filter radiometer housing, the cover of which has been removed for easy viewing. In the picture, only one DFU is mounted. In total the filter radiometer can hold three DFUs, for UV-VIS, NIR and SWIR.

Fig. 3. Photograph of the complete system, set up to measure the spectral irradiance of a FEL lamp. From front to back: electronics box with controlling laptop, FEL lamp, external baffles to shield for stray light and filter radiometer.

III.   CALIBRATION

The UV-VIS DFU was calibrated on the Absolute Cryogenic Radiometer (ACR) facility at VSL, which is the primary standard for radiometry in the Netherlands [5,12]. Fig. 4 shows an overview of this facility, the heart of which is an ESCR. Performance of the ACR facility has been well established in international comparisons [13,14]. The ACR features several light sources, to cover the full wavelength range from UV to SWIR. The radiation of the selected light source is sent into a double-monochromator system (subtractive mode) to disperse the radiation into its spectral components. The output of the second monochromator is sent through an optical high-pass filter to remove any remaining higher order spectral components. The radiation then passes through an optical shutter, which can be closed for dark measurements. Mirror optics is then used to form a spot with a diameter of approximately 4.5 mm and an opening angle of f/8. This spot can directed onto the ESCR to determine the spectral radiant flux, or onto a transfer detector that has been previously calibrated against the ESCR.
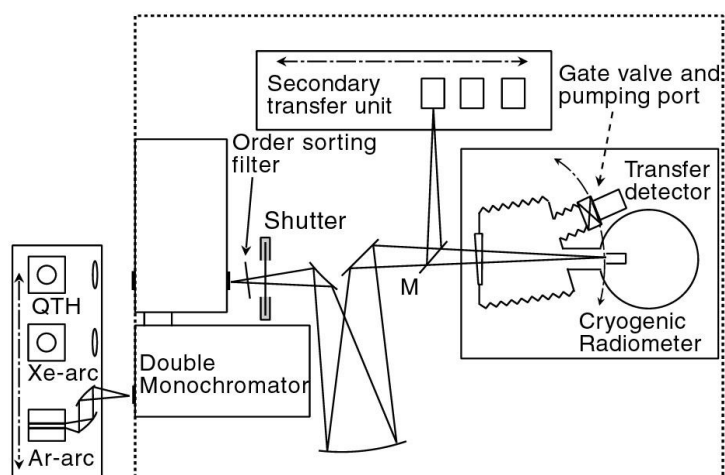

Fig. 4. Layout of the ACR facility, which is the primary standard for radiometry in the Netherlands. Recently a laser driven light source (LDLS) was added to the available light sources, which is not shown in the picture.

A mirror (denoted M in fig. 4) can be used to direct the light onto a secondary transfer unit. The transfer unit can be scanned in two dimensions (x and y) perpendicular to the incoming beam. Our scanning spot method [15,16] allows us to determine the spectral irradiance responsivity of an unknown detector by scanning a spot over the active area of the detector, without requiring either the spot or the detector sensitivity to be spatially uniform. Also, the area of the detector aperture need not be known beforehand. The spectral irradiance responsivity of the detector $S(\lambda)$ can be calculated according to

$$S(\lambda) = \iint \frac{R_{st}(\lambda)\varphi_d(x, y)}{\varphi_{st}(x, y)}\, \mathrm{d}x\mathrm{d}y \tag{1}$$

where $R_{st}(\lambda)$ is the known spectral flux responsivity of a standard detector previously calibrated against the ESCR, $\varphi_d(x, y)$ the signal measured for the unknown detector at scan position (x, y) and $\varphi_{st}(x, y)$ that for the standard. In the case of the filter radiometer, the unknown detector is the DFU, which for each channel is a combination of a (trap) detector and a band-pass filter. It was decided to calibrate the combination rather than the separate elements, so that the interactions between the elements and the way their inhomogeneities add up are automatically taken care of. The calibration thus results in a set of spectral irradiance responsivity curves $S_i(\lambda)$, one for each filter i in the DFU.

The uncertainty budget for the DFU calibration on the ACR is given in table 2 for three representative channels, with wavelengths near the beginning, middle and end of the UV-VIS range. Details on the uncertainty estimation method are given in [15].

Contribution	Standard uncertainty		
	280 nm	**540 nm**	**900 nm**
Amplification factor standard	0.002%	0.002%	0.002%
Amplification factor detector	0.000%	0.000%	0.000%
Responsivity standard	0.503%	0.058%	0.076%
Step size	0.416%	0.410%	0.410%
Numerical approximation	0.000%	0.000%	0.000%
Non-orthogonality of x and y axes	0.061%	0.061%	0.061%
Variation in irradiance due to misalignment of scan plane and detector plane	0.005%	0.005%	0.005%
Stray light	0.010%	0.010%	0.010%
Wavelength error	0.435%	0.057%	0.013%
Angular alignment of detector	0.333%	0.333%	0.333%
Combined	0.854%	0.538%	0.537%

Table 2. Uncertainty budget for the calibration of the DFU on the ACR facility, for three representative channels indicated by their respective nominal wavelengths.

IV.   FITTING OF IRRADIANCE SPECTRA

If we use the filter radiometer to measure a broad-band light source, we will get a dark-subtracted measurement signal φ_i for each filter i. For ideal filters, with infinitesimal small band width $\Delta\lambda_i$, the source spectral irradiance $E(\lambda_i)$ at the channel wavelength λ_i can then be constructed from the measured signal via the simple relation $E(\lambda_i) = \varphi_i / (S_i(\lambda_i)\Delta\lambda_i)$. Subsequently, a model of the irradiance distribution $E_{\text{model}}(\lambda, \mathbf{p})$ containing a number of model parameters $\mathbf{p}$ can be fitted through the measured spectral irradiances to obtain the spectral irradiance at intermediate wavelengths. However, the actual filters in the filter radiometer have finite bandwidths, as do all practical filters, so that the spectral irradiance $E(\lambda)$ may not be treated as constant within the filter bandwidth. The measured signal in volts is built up from contributions over the full wavelength range over which the combination of filter and detector has a non-zero responsivity:

$$\varphi_i = \int S_i(\lambda)E(\lambda)\,\mathrm{d}\lambda . \tag{2}$$

In order to find the spectral irradiance distribution from the measured signals, $E(\lambda)$ is replaced by the model distribution $E_{\text{model}}(\lambda, \mathbf{p})$ in (2) to obtain a modelled signal $\varphi_{\text{model},i}(\mathbf{p})$. The absolute difference $|\varphi_i(\mathbf{p}) - \varphi_{\text{model},i}(\mathbf{p})|$ is then minimized as a function of $\mathbf{p}$ over all channels i in a Levenberg-Marquardt fit procedure. Note that in each iteration of the Levenberg-Marquardt algorithm, the integral (2) is evaluated. From the optimized parameters $\tilde{\mathbf{p}}$, the spectral irradiance at each wavelength can be obtained by the substitution $E(\lambda) = E_{\text{model}}(\lambda, \tilde{\mathbf{p}})$.

For fitting the spectral irradiance of FEL lamps, a modified Planckian spectrum was chosen [7]:

$$E_{\text{FEL}}(\lambda, T, b_0, \ldots, b_m) = \frac{\sum_{n=1}^{m} b_n \lambda^n}{\lambda^5 [\exp(c/\lambda T) - 1]} . \tag{3}$$

Here T is the temperature of the Planckian radiator and $c = 1.4388$ mK a constant. The polynomial in the numerator expresses the fact that the emissivity is not constant with wavelength. The choice of polynomial order

is a compromise between the closeness of fit at the position of the filter channels and the stability of the fitted curve in between channels. With the filters currently implemented in the UV-VIS DFU, it was found that a third-order polynomial gave the best results.

V.   PERFORMANCE VERIFICATION

To verify the performance of the filter radiometer in UV-VIS, verification measurements using FEL lamps with known spectral irradiance were performed. The FEL lamps have been calibrated for spectral irradiance on the Spectral Irradiance facility (SIRF) of VSL [17]. The verification setup is depicted schematically in fig. 5. The 1000 W FEL lamps were placed at a distance of 50 cm from the filter radiometer aperture, with two baffles with circular apertures in between to shield stray light and a third baffle under 45º behind to reduce back reflections. Alignment of the filter radiometer and the apertures is done with the aid of a laser, and the distance is measured with a measuring rod. Each verification measurement consists of a dark measurement and 30 measurements per selected filter. In between filters there is a 3 s transition time for mechanical changeover of the filter and stabilization of the signal.
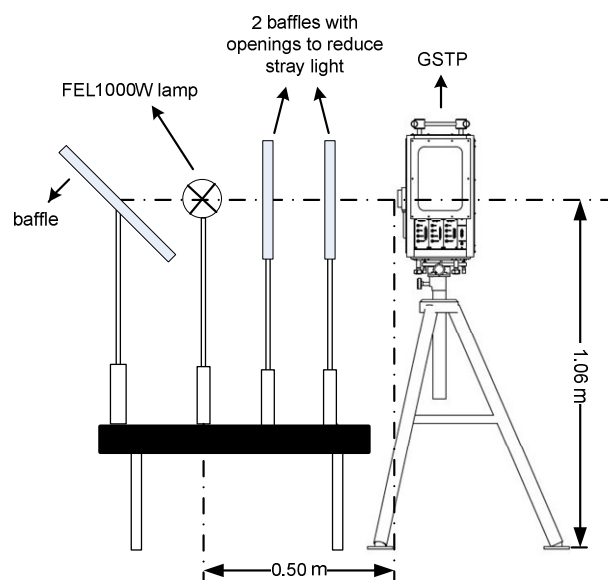

Fig. 5. Setup used for the performance verification measurements.

The results of the verification experiment were evaluated by comparing the fitted spectral irradiance based on the filter radiometer measurements to the known spectral irradiance of the FEL lamps. In fig. 6, the relative difference in spectral irradiance for one lamp is plotted. The fitted irradiance spectrum $E_{\text{model}}(\lambda_i, \tilde{\mathbf{p}})$, based on a third order polynomial model according to (3), is evaluated at the nominal channel wavelengths λ_i and then compared to the known spectral irradiance of the calibrated FEL lamp $E_{\text{ref}}(\lambda_i)$. A combined expanded uncertainty $U(E_{\text{model}}(\lambda_i, \tilde{\mathbf{p}}) - E_{\text{ref}}(\lambda_i))$ at 95% level of confidence was calculated for the difference $E_{\text{model}}(\lambda_i, \tilde{\mathbf{p}}) - E_{\text{ref}}(\lambda_i)$, and is indicated in fig. 6. This uncertainty involves four contributions: the uncertainty of the filter radiometer from its calibration, the uncertainty of the reference spectrum, the uncertainty coming from the verification experiment itself (alignment, distance, stray light and reproducibility) and the uncertainty connected to the fitting procedure.
The ratio

$$E_{\text{n},i} = \frac{E_{\text{model}}(\lambda_i, \tilde{\mathbf{p}}) - E_{\text{ref}}(\lambda_i)}{U(E_{\text{model}}(\lambda_i, \tilde{\mathbf{p}}) - E_{\text{ref}}(\lambda_i))}. \tag{4}$$

indicates whether the observed difference between measurement and reference is consistent with the estimated uncertainty. A successful verification result (to the stated level of confidence) requires that $|E_{n,i}| \leq 1$. This is indeed the case for all channels in fig. 6.
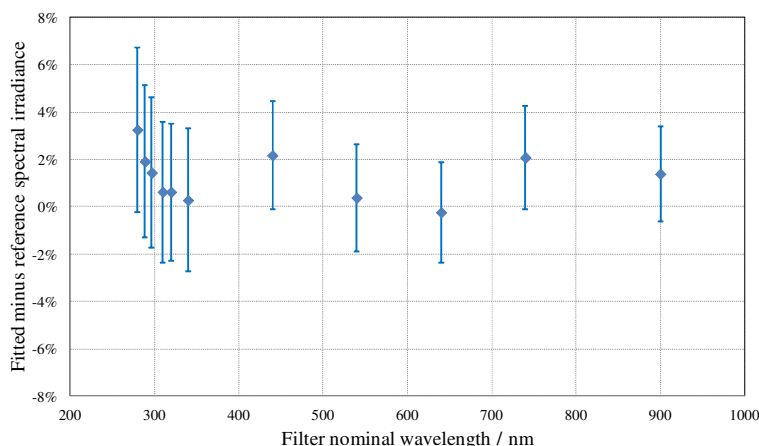

Fig. 6. Relative difference between fitted and reference spectral irradiance. The error bars denote the uncertainty at 95% level of confidence ($k = 2$).

VI.   CONCLUSION AND OUTLOOK

We have designed a filter radiometer as a portable traceability solution for the on-site calibration of light sources used in the ground-based calibration of earth observation instruments. The module for the UV-VIS subrange was realized and calibrated against the primary standard of radiometry in the Netherlands. Performance verification against known FEL lamps showed deviations consistent with the estimated uncertainties. The filter radiometer itself has a standard uncertainty of 0.54-0.86% depending on the channel. The intention is to extend the project with the realization of the NIR and SWIR modules.

ACKNOWLEDGEMENT

REFERENCES

[1]   G. Ohring (ed.), *Achieving Satellite Instrument Calibration for Climate Change (ASIC3)*, 2007
[2]   Bureau International des Poids et Mesures, *The International System of Units (SI)*, 8th ed., 2008
[3]   J. E. Martin, N. P. Fox, and P. J. Key, "A cryogenic radiometer for absolute radiometric measurements," *Metrologia*, 21, pp. 147–155, 1985
[4]   T. R. Gentile, J. M. Houston, J. E. Hardis, C. L. Cromer, and A. C. Parr, "National Institute of Standards and Technology high-accuracy cryogenic radiometer", *Appl. Opt.*, 35, pp. 1056-1068, 1996
[5]   C. A. Schrama, R. Bosma, K. Gibb, H. Reijn and P. Bloembergen, "Comparison of monochromator-based and laser-based cryogenic radiometry", *Metrologia*, 35, pp. 431-435, 1998
[6]   N. P. Fox, "Trap Detectors and their Properties", *Metrologia*, 28, pp. 197-202, 1991
[7]   P. Karha, P. Toivanen F. Manoocheri and E. Ikonen, "Development of a detector-based absolute spectral irradiance scale in the 380nm to 900nm spectral range", *Appl. Opt.*, 36, pp. 8909-8918, 1997
[8]   P. Toivanen, F. Manoochehri, P. Karha, E. Ikkonen, A. Lassila, "Method for characterization of filter radiometers", *Appl. Opt.*, 38, pp. 1709-1713, 1999

[9] T. Kubarsepp, P. Karha, F. Manoocheri, S. Nevas, L. Ylianttila and E. Ikonen, "Spectral irradiance measurements of tungsten lamps with filter radiometers in the spectral range 290 nm to 900 nm", *Metrologia*, 37, pp. 305-312, 2000

[10] M. Durak, F. samadov, "Realization of a filter radiometer-based irradiance scale with high accuracy in the region from 286 nm to 901 nm", *Metrologia*, 41, pp. 401-406, 2004

[11] Y. J. Liu, G. Xu, M. Ojanen, E. Ikonen, "Spectral irradiance comparison using a multi-wavelength filter radiometer", *Metrologia*, 46, pp. 181-185, 2009

[12] C. A. Schrama, P. Bloembergen and E. W. M. Van der Ham, "Monochromator-based cryogenic radiometry between 1 μm and 20 μm", *Metrologia*, 37, 567-570, (2000)

[13] S. Brown, T. Larason, and Y. Ohno, *Report on the Key Comparison CCPR-K2.a-2003 Spectral Responsivity in the Range of 900 nm to 1600 nm*, BIPM, 2003 (available from kcdb.bipm.org)

[14] R. Goebel, M. Stock, *Report on the key comparison CCPR-K2.b of spectral responsivity measurements in the wavelength range 300 nm to 1000 nm*, BIPM, 2004 (available from kcdb.bipm.org)

[15] C.A. Schrama, H. Reijn, "Novel calibration method for filter radiometers", *Metrologia*, 36, pp. 179-182, 1999

[16] C. A. Schrama, E. W. M. Van der Ham, "Sampling period criterion in a scanning-beam technique", *Appl. Opt.*, 39, pp. 1500-1504, 2000

[17] E.W.M. van der Ham, H. C. D. Bos and C. A. Schrama, "Primary realization of a spectral irradiance scale employing monochromator-based cryogenic radiometry between 200 nm and 20μm", *Metrologia*, 40, pp. 177-180, 2003